International Journal of Applied Power Engineering (IJAPE)
Vol. 15, No. 2, June 2026, pp. 546~553
ISSN: 2252-8792, DOI: 10.11591/ijape.v15.i2.pp546-553

Utilization of BSA optimized cascade controller in a renewable energy-based AGC systems

Rambabu Kasukurthi, R. Srinu Naik
Department of Electrical Engineering, Andhra University College of Engineering, Andhra University, Visakhapatnam, India

Article Info

Article history:

Received May 7, 2025
Revised Dec 21, 2025
Accepted Mar 12, 2026

Keywords:

Automatic generation control
Automatic voltage regulation
Bird swarm algorithm
PID-TID controller
Wind turbine systems

ABSTRACT

A novel cascade controller named proportional integral derivative-tilt integral derivative (PID-TID) is proposed for a two-area thermal-wind automatic generation control (AGC) system and its gains are optimized by a novel metaheuristic bird swarm algorithm (BSA). The BSA tuned PID-TID controller enhances dynamics over PID and TID controller in terms of settling time and peak shoots. Moreover, dynamics with wind integration have shown significant improvement over thermal system alone. Further system has shown enhanced dynamics with redox flow batteries (RFB) over thermal-wind system. Furthermore, studies with automatic voltage regulation (AVR) strengthen voltage stability. Also, responses with PID-TID have shown steady dynamic profile at various loading conditions. Integrating wind energy into thermal system results in significant enhancements in dynamics showcasing greater stability. Also, improvements are evident with the RFB introduction, enhance dynamic with in hybrid system. The incorporation of AVR enhance voltage stability. The proposed PID-TID demonstrates significant robustness ensuring stable response under loading condition and effectively boost dynamic performance.

Corresponding Author:

Rambabu Kasukurthi
Department of Electrical Engineering, Andhra University College of Engineering, Andhra University
Visakhapatnam, India
Email: rambabu.kasukurthi@gmail.com

1. INTRODUCTION

Balancing of power has become challenge due to increase in grid's size and complexity. Also, keeping the system stable at permissible limits has become difficult. This issue can be addressed by automatic generation control (AGC) that maintains frequency, voltage and power in permissible limits [1], [2]. AGC works initiated by one area and broaden to complicated multi-area systems [3]-[5] considering nonlinearities like GDB, delay, and GRC. Further, frequency-voltage coupling exists due to interaction of AGC with automatic voltage regulator (AVR) loops [1], [2], [5]. The efficient integration of renewables including solar and wind turbine systems (WTS), is studied in AGC [6]-[8]. The study in [9], [10] examined WTS with constant wind velocity. However, because of intrinsic wind changes, WTS production is variable. The incorporation of WTS into AGC-AVR framework has not received much attention, although it reduces this intermittency.

Power system performance deteriorates under faulty conditions leading to transients worsening system dynamics. This issue can be mitigated by the energy storage device (ESD) integration [10], [11]. ESD such as redox flow battery (RFB) and its advantages in AGC studies are noted in [10]. These findings can be extended to more complex configurations, such as two-area systems, particularly when integrating renewable energy sources.

The advancement of the auxiliary controller has been the primary focus of AGC research. Basic fractional [12], cascade and tilt controllers such as proportional integral derivative (PID) [13], PI-PD [14], tilt integral derivative (TID) [15], fuzzy [16], and sliding controller [17] have been introduced over time. However, a novel combination such as PID-TID for two-area AGC-AVR with RS has not been investigated.

Recent developments in AGC research have shown that many metaheuristic methods are successfully applied, such as swarm [15], crow search [18], hybrid crow search [19], genetic [20], antlion [21], and cuckoo search [22]. Meng *et al*. [23] introduced an optimization technique known as the BSA, inspired by the cooperative foraging behavior of birds. The algorithm effectively achieves global optimization with fewer iterations, offering high accuracy and fast convergence. Also, BSA has significantly improved dynamics of AGC systems [24], [25]. Yet the impact of BSA on AGC-AVR is to be evaluated.

Sensitivity analysis is commonly employed in AGC to evaluate the controller robustness against substantial load oscillations in the system [19], [25]. While this work introduces a novel controller, termed TIDN, a sensitivity analysis has yet to be performed. This presents an opportunity for further research. The following objectives have been outlined and are: i) to develop a two-area AGC system incorporating thermal, WTS components; ii) implement several controllers like TID, PID, and cascaded of PID and TID (PID-TID), in system model (Figure 1); iii) employing BSA for concurrent optimization; iv) assessment of system dynamics due to WTS integration; v) evaluation of system dynamic performance with ESD integration; vi) sensitivity-based robustness assessment, and vii) to study the impact of AVR loop on WTS-thermal-ESD system.

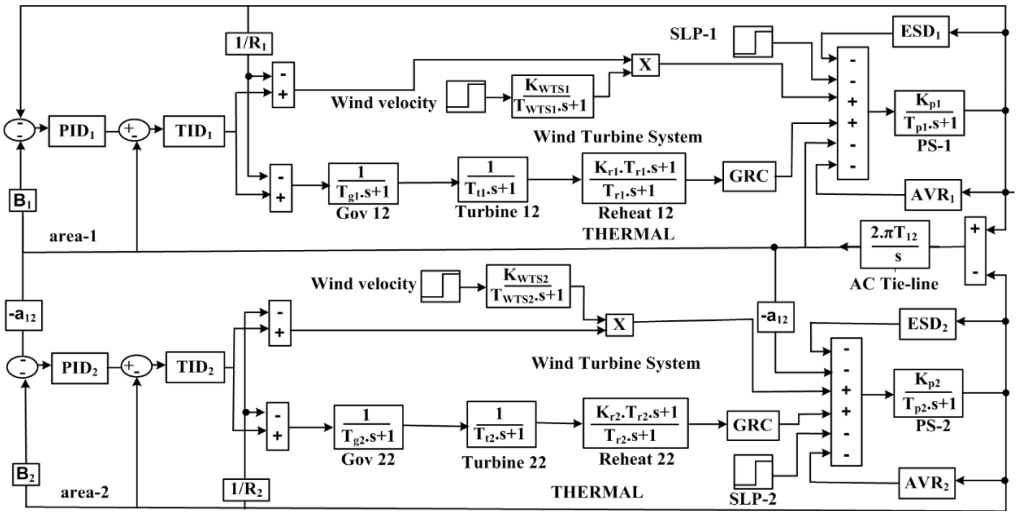

Figure 1. Proposed system model

2. SYSTEM DESCRIPTION

2.1. Proposed controller

An innovative controller that combines both integer and fractional controllers is the tilt controller, first introduced in [6]. While the structures of PID and TID controllers are similar, the TID controller introduces a scaling factor of 1/sn to the proportional term of the PID. However, incorporating derivative control within the forward path can lead to the undesired phenomenon of derivative kick in electronic systems [6]. The cascading PID and TID controllers provide fast and stable frequency regulation. PID handles rapid deviations, while TID addresses slower disturbances, together improving stability, reducing overshoot, and enhancing overall system performance. The equations of PID, PID, and the cascaded PID-TID are in (1)-(3) respectively.

$$F_1(s) = \mathrm{K}_{KP_i} + \frac{K_{\mathrm{KI}_i}}{s} + \mathrm{K}_{\mathrm{KD}_i} s \quad (1)$$

$$F_2(s) = \frac{K_{KT_i}}{1/s^{n_{Ki}}} + \frac{K_{\mathrm{KI}_i}}{s} + \mathrm{K}_{\mathrm{KD}_i} s \quad (2)$$

$$F_{PID\text{-}TID}(s) = \mathrm{F}_1(s) + \mathrm{F}_2(s) \quad (3)$$

2.2. Bird swarm algorithm

Meng *et al*. [23] proposed a swarm intelligence algorithm with bird flock behavior named BSA. The algorithm models the intelligence of birds based on key behaviors such as foraging, flying, and maintaining alertness. BSA primarily simulates bird movements through three strategies: i) searching for food, ii) staying alert in response to potential threats, and iii) escaping from predators. Foraging behavior in BSA is represented in (4), where birds move toward their personal best and the global best positions to exploit promising solutions.

$$X_{p,q}^{i+1} = X_{p,}^{i} + (P_{p,q} - X_{p,q}^{m}) \times D \times rand_j(0,1) \ + (g_p - X_{p,q}^{i}) \times t \times rand_j(0,1) \quad (4)$$

Where position (x), dimension (q), birds count (p), past position (PP), random (rand), social (t), and cognitive (P) coefficients. Flight behavior in (5) and (6) uses flight lengths (fl = 0–2) and alternating roles to explore new regions of the search space.

$$X_{p,q}^{i+1} = X_{p,q}^{i} + A_1(mean_q - X_{p,q}^{m}) \times rand_i(0,1) \ + A_2(P_{p,q} - X_{p,q}^{m}) \times rand_i(-1,1) \quad (5)$$

$$X_{p,q}^{j+1} = X_{p,q}^{n} + randn_i(0,1) \times X_{p,q}^{j} \quad (6)$$

Vigilance behavior in (7) describes how birds at the swarm's edge stay alert to reduce predator risk. It flowchart is in Figure 2.

$$X_{p,q}^{i+1} = X_{p,q}^{j} + (X_{p,q}^{j} - X_{p,q}^{j}) \times fll \times rand_i(0,1) \quad (7)$$

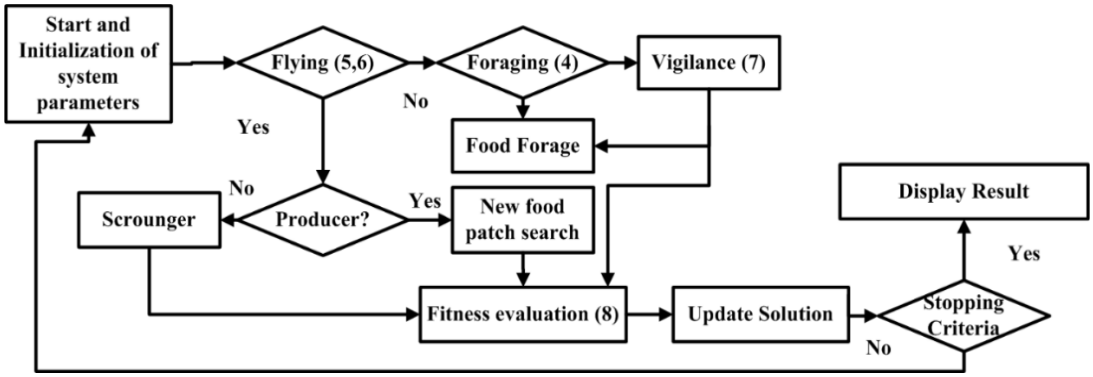

Figure 2. BSA working diagram

3. INVESTIGATED SYSTEM

The transfer function model of a two-area thermal system is integrated with a WTS, is in Figure 1. The system's nominal parameters, derived from references [8], [20], are detailed in the appendix. The WTS, RFB, and AVR loops are simplified into low-order linear models. WTS has a rigid rotor with power responding linearly to frequency changes, assuming nearly constant wind. RFB uses linear governor and turbine dynamics with reheat delay, ignoring nonlinearities. System dynamics are analyzed by using PID, TID, and PID-TID controller in a thermal-wind-RFB-AVR system. Controller gains are optimized by BSA technique considering ISE as performance index in (8).

$$\eta_{\text{ISE}} = \int_0^t \{(\Delta \text{F}_m)^2 + (\Delta \text{P}_{\text{m-n}})^2\}.\text{dt} \quad (8)$$

Nominal values are: WTS: K_{WTS} = 1.25, T_{WTS} = 0.041 s; Thermal system: F_i = 60 Hz, B_i = 0.425 MW p.u., H_i = 5.00 s, T_{ij} = 0.0860 p.u. MW/rad, T_{gi} = 0.080 s, Kp_i = 120 Hz/p.u., R_i = 2.4 Hz/p.u., Bi = 0.425 MW/Hz, Tp_i = 20 s, , Tt_i = 0.3 s, Kr_i = 0.5, Tr_i = 10 s; and RFB as ESD: K_{RFB} = 1.0, T_{RFB} = 0.01 s.

4. ANALYSIS OF SIMULATION RESULTS

4.1. Controllers' assessment

Thermal system in Figure 1 is studied with PID, TID, and PID-TID controllers independently. The gains of these controllers are enhanced by BSA, with the optimal values provided in Table 1. Comparison of

the controller dynamics is shown in Figure 3(a). Table 2 summarizes the performance indicators, including POS, PUS, and ST, which are derived from the results depicted in Figure 3(a).

A comprehensive examination of Figure 3(a), along with the performance metrics in Table 2, indicates the PID-TID controller demonstrates superior dynamics over the PID and TID controllers and is utilized for the remainder of the studies. The PID-TID controller was tuned using BSA with different performance indices, and Figure 3(b) shows that ISE yields the best improvement in system dynamics.

Table 1. Optimum PID, TID, and PID-TID controller values

Controller	Optimal values
PID	K_{KP1}^* = 0.5300, K_{KI1}^* = 0.2090, K_{KD1}^*= 0.2402, K_{KP2}^* = 0.6004, K_{KI2}^* = 0.2087, K_{KD2}^*= 0.2140
TID	K_{KT1}^* = 0.730, K_{KI1}^* = 0.3021, K_{KD1}^* = 0.2450, N_{K1}^*= 92.520, n_{K1} = 4.420, K_{KT2}^* = 0. 7341, K_{KI2}^* = 0.2940, K_{KD2}^* = 0.2501, N_{K2}^*= 92.620, n_{K2}^* = 4.360
PID-TID	K_{KP1}^* = 0.6600, K_{KI1}^* = 0.2090, K_{KD1}^*= 0.2342, K_{KP2}^* = 0.5990, K_{KI2}^* = 0.2072, K_{KD2}^*= 0.2391, K_{KT1}^* = 0.683, K_{KI1}^* = 0.2730, K_{KD1}^*= 0.2105, n_{K1} = 4.600, K_{KT2}^* = 0.6180, K_{KI2}^* = 0.2050, K_{KD2}^*= 0.2016, n_{K2}^* = 4. 601

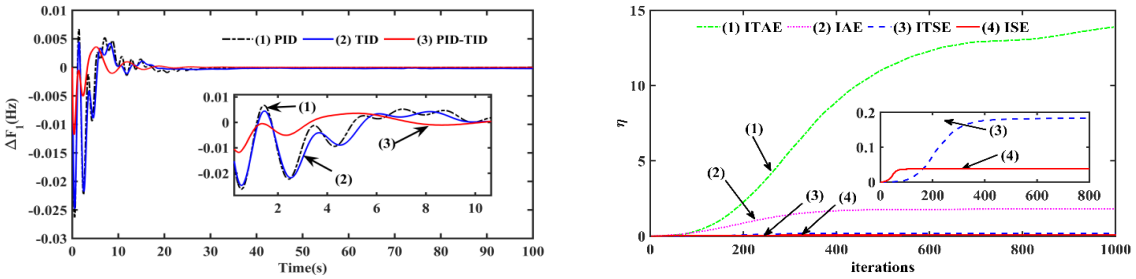

Figure 3. Performance comparison of control strategies: (a) for PI, PID, and PID–TID controller comparisons and (b) comparisons with various indices

Table 2. System dynamic performance comparison from Figure 3

Responses	Indices	PID-TID	PID	PI
ΔF_1	POs	0.0035	0.0044	0.0067
	PUs	0.0116	0.0247	0.0260
	ST	37.990	46.860	53.700

4.2. Comparison with various algorithms

Various algorithms such as BSA, flower pollination algorithm and cuckoo search are considered with metrics such as convergence rate are evaluated. Figure 4(a) shows the simulation results for the three algorithms, with convergence analysis confirming the BSA algorithm's superiority in optimizing the PID-TID controller. The results demonstrate BSA's potential to enhance convergence rate and accuracy in power system optimization.

4.3. Evaluation of WTS integration impact on system performance

In Case-4.1, the system under investigation is amalgamated with WTS. The PID-TID controller, identified as the best performer in Case-4.1, is employed and is optimized by BSA. The optimal PID-TID parameters are in Table 3. The dynamic comparison is made with the thermal unit in Figure 4(b). It clearly indicates that the integration of WTS leads to enhanced dynamic performance.

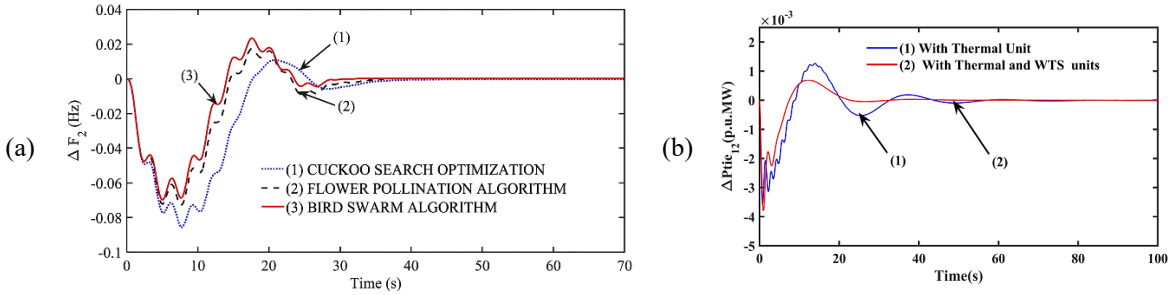

Figure 4. Dynamic comparisons: (a) algorithm comparisons and (b) with and without WTS units

Table 3. Optimum values of the PID-TID controller considering WTS unit

Parameter	Value	Parameter	Value	Parameter	Value
K_{KP1}^*	0.6800	K_{KI1}^*	0.2205	K_{KD1}^*	0.2472
K_{KP2}^*	0.6200	K_{KI2}^*	0.2088	K_{KD2}^*	0.2410
K_{KT1}^*	0.6895	K_{KI1}^*	0.3001	K_{KD1}^*	0.2178
n_{K1}	4.580	K_{KT2}^*	0.6310	K_{KI2}^*	0.2086
K_{KD2}^*	0.2210	n_{K2}^*	4.001		

4.4. Evaluation of ESD integration on system dynamics

Section 4.3 explores the integration of RFB into the system, considering the PID-TID controller adjusted by BSA, with the optimal values in Table 4. The dynamics with and without ESD are illustrated in Figure 5. From Figures 5(a) and 5(b), the system with the ESD link exhibits significantly better dynamic performance compared to the system without it.

Table 4. Optimal PID-TID controller with ESD

Parameter	Value	Parameter	Value	Parameter	Value
K_{KP1}^*	0.6905	K_{KI1}^*	0.2278	K_{KD1}^*	0.2494
K_{KP2}^*	0.6507	K_{KI2}^*	0.2280	K_{KD2}^*	0.2500
K_{KT1}^*	0.7070	K_{KI1}^*	0.3100	K_{KD1}^*	0.2202
n_{K1}	5.002	K_{KT2}^*	0.6440	K_{KI2}^*	0.2100
K_{KD2}^*	0.2415	n_{K2}^*	5.300		

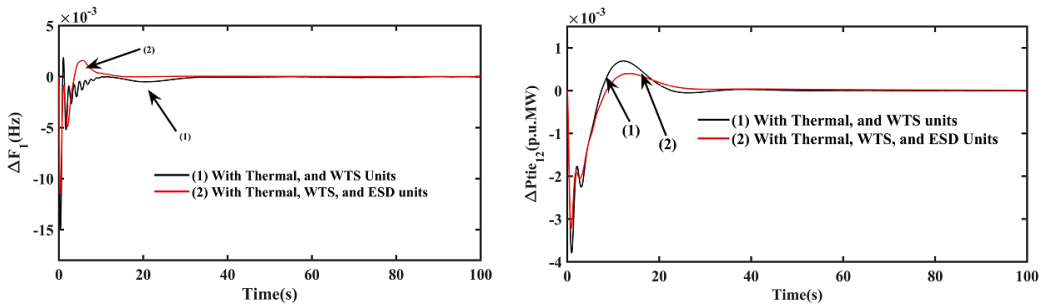

(a) (b)

Figure 5. System performance with and without ESD integration: (a) ΔF_1 and (b) $\Delta Ptie_{12}$

4.5. Sensitivity analysis

To estimate the sturdiness of the top-performing PID-TID controller from Case Study-A, we consider two loading scenarios—25% and 75%—by varying the system load by ±25% from the nominal 50% loading. After applying BSA, the optimal controller settings for each scenario are presented in Table 5. Figures 6(a) and 6(b) compare and illustrate the system dynamics for three load scenarios: 25%, 50%, and 75%. The PID-TID controller consistently maintains strong performance, even with load deviations of ±25% from the nominal value, as shown by the dynamic responses. This demonstrates that the PID-TID controller offers stable performance across a range of system loading conditions.

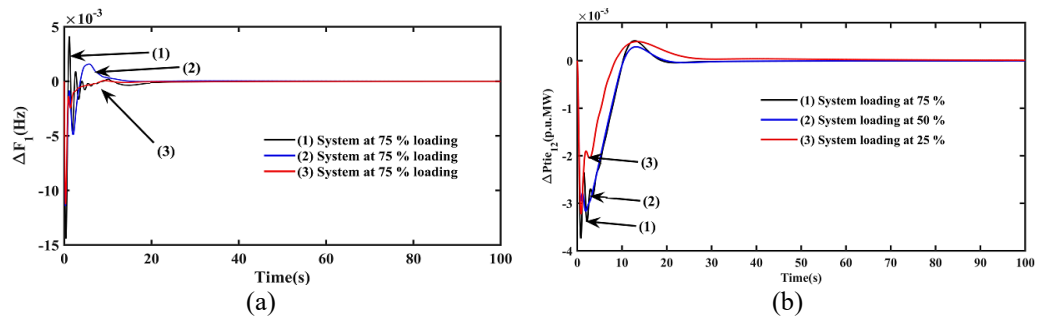

(a) (b)

Figure 6. System performance at different loading: (a) ΔF_1 and (b) $\Delta P_{tie1\text{-}2}$

4.6. Impact of AVR loop on WTS-thermal-ESD system

Figure 1 with RFB-WTS-thermal is integrated with AVR and is under study. A thermal power plant, wind unit, RFB, and AVR loop are considered. BSA optimized the PID-TID gains, plotting their responses in Figure 7. The responses in Figures 7(a) and 7(b) suggest the AVR loop outcomes over AGC system by enhancing voltage and frequency stability.

Table 5. Control settings of PID-TID at varied loading

Loading	Parameter	Value	Parameter	Value	Parameter	Value
At 25 %	K_{KP1}^*	0.6250	K_{KI1}^*	0.1990	K_{KD1}^*	0.2020
	K_{KP2}^*	0.5900	K_{KI2}^*	0.1990	K_{KD2}^*	0.2210
	K_{KT1}^*	0.6350	K_{KI1}^*	0.2605	K_{KD1}^*	0.2000
	n_{K1}	3.9900	K_{KT2}^*	0.6050	K_{KI2}^*	0.2000
	K_{KD2}^*	0.2011	n_{K2}^*	4.000		
At 75 %	K_{KP1}^*	0.6850	K_{KI1}^*	0.2500	K_{KD1}^*	0.2402
	K_{KP2}^*	0.6000	K_{KI2}^*	0.2326	K_{KD2}^*	0.2498
	K_{KT1}^*	0.6550	K_{KI1}^*	0.2860	K_{KD1}^*	0.2200
	n_{K1}	4.850	K_{KT2}^*	0.6550	K_{KI2}^*	0.2230
	K_{KD2}^*	0.2210	n_{K2}^*	4.500		

(a)

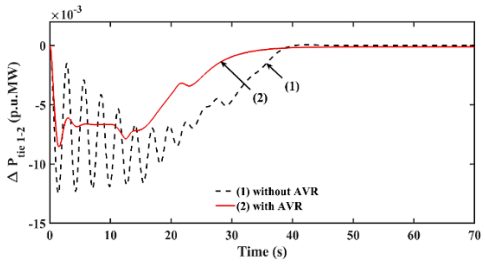

(b)

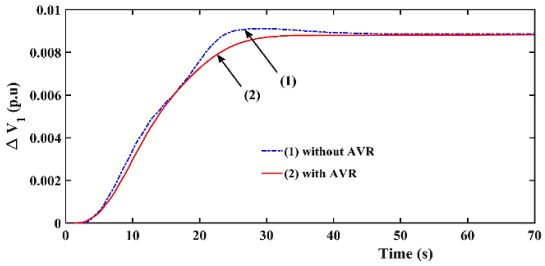

Figure 7. Impact of AVR: (a) $\Delta P_{tie1\text{-}2}$ and (b) ΔV_1

5. CONCLUSION

An effort was made to improve the recital of a two-area AGC system by employing various secondary controllers, including PID-TID, PID, and TID controllers. The characteristics of these tilt controllers were optimized using the BSA. The results indicated that the PID-TID controller outperforms over others when comparing the dynamics. The integration of Wind units enhanced the dynamics of the two-area thermal system compared to a system without renewable sources. Additionally, the inclusion of a redox batteries further improved system performance. The sensitivity study confirmed that the PID-TID controller maintains stable performance across a broad range of system loading scenarios, eliminating the need to modify the original parameter values. Furthermore, studies with AVR have shown significant improvement in system dynamics. Future directions include hardware-in-the-loop testing, extending to hybrid renewable systems, and comparing performance with other metaheuristic optimization algorithms.

FUNDING INFORMATION

No funding involved.

AUTHOR CONTRIBUTIONS STATEMENT

This journal uses the Contributor Roles Taxonomy (CRediT) to recognize individual author contributions, reduce authorship disputes, and facilitate collaboration.

Name of Author	C	M	So	Va	Fo	I	R	D	O	E	Vi	Su	P	Fu
Rambabu Kasukurthi	✓	✓	✓	✓	✓	✓		✓	✓	✓			✓	
R. Srinu Naik		✓				✓		✓	✓	✓	✓	✓		

C : **C**onceptualization
M : **M**ethodology
So : **So**ftware
Va : **Va**lidation
Fo : **Fo**rmal analysis
I : **I**nvestigation
R : **R**esources
D : **D**ata Curation
O : Writing - **O**riginal Draft
E : Writing - Review & **E**diting
Vi : **Vi**sualization
Su : **Su**pervision
P : **P**roject administration
Fu : **Fu**nding acquisition

CONFLICT OF INTEREST STATEMENT

No conflict of interest.

INFORMED CONSENT

We have obtained informed consent from all individuals included in this study.

ETHICAL APPROVAL

The research related to animal use has been complied with all the relevant national regulations and institutional policies for the care and use of animals.

DATA AVAILABILITY

Data availability is not applicable to this paper as no new data were created or analyzed in this study.

REFERENCES

[1] N. R. Babu, S. K. Bhagat, L. C. Saikia, T. Chiranjeevi, R. Devarapalli, and F. P. G. Márquez, "A comprehensive review of recent strategies on automatic generation control/load frequency control in power systems," *Archives of Computational Methods in Engineering*, vol. 30, no. 1, pp. 543–572, Jan. 2023, doi: 10.1007/s11831-022-09810-y.

[2] S. K. Bhagat, N. R. Babu, L. C. Saikia, T. Chiranjeevi, R. Devarapalli, and F. P. G. Márquez, "A review on various secondary controllers and optimization techniques in automatic generation control," *Archives of Computational Methods in Engineering*, vol. 30, no. 5, pp. 3081–3111, Jun. 2023, doi: 10.1007/s11831-023-09895-z.

[3] T. Chiranjeevi *et al.*, "Impact of HVDC link and electric vehicle on multi-area power system using MOA optimized I-TD2N controller," *Results in Engineering*, vol. 25, p. 103901, Mar. 2025, doi: 10.1016/j.rineng.2024.103901.

[4] A. Saha, P. Dash, T. Chiranjeevi, and N. R. Babu, "Implementation of combined hydrogen aqua electrolyser-fuel cell and redox-flow-battery under restructured situation of AGC employing TSA optimized PDN(FOPI) controller," *Journal of Taibah University for Science*, vol. 18, no. 1, Dec. 2024, doi: 10.1080/16583655.2024.2334004.

[5] S. Bhagat, N. Babu, L. Sakia, and D. Raju, "Maiden application of meta-heuristic techniques with optimized integral minus tilt-derivative controller for AGC of multi-area multi-source system," *ICST Transactions on Scalable Information Systems*, p. 164557, Jul. 2018, doi: 10.4108/eai.13-7-2018.164557.

[6] S. K. Bhagat, L. C. Saikia, and N. R. Babu, "Mitigation of AGC problem of the RES integrated hydro-thermal system using FACTS and INEC based AHVDC with ESS considering the 3DOF-TIDN controller," *IETE Journal of Research*, vol. 70, no. 4, pp. 3964–3984, Apr. 2024, doi: 10.1080/03772063.2023.2210539.

[7] Z. Huang and W. Wu, "Dual-stage MPC-based AGC for wind farm considering aerodynamic interactions," *IEEE Transactions on Sustainable Energy*, vol. 16, no. 2, pp. 1098–1113, Apr. 2025, doi: 10.1109/TSTE.2024.3502518.

[8] Y. Xu, F. Li, Z. Jin, and M. Hassani Variani, "Dynamic gain-tuning control (DGTC) approach for AGC with effects of wind power," *IEEE Transactions on Power Systems*, vol. 31, no. 5, pp. 3339–3348, Sep. 2016, doi: 10.1109/TPWRS.2015.2489562.

[9] W. Tasnin and L. C. Saikia, "Maiden application of an sine–cosine algorithm optimised FO cascade controller in automatic generation control of multi-area thermal system incorporating dish-Stirling solar and geothermal power plants," *IET Renewable Power Generation*, vol. 12, no. 5, pp. 585–597, Apr. 2018, doi: 10.1049/iet-rpg.2017.0063.

[10] A. Saha and L. C. Saikia, "Combined application of redox flow battery and DC link in restructured AGC system in the presence of WTS and DSTS in distributed generation unit," *IET Generation, Transmission and Distribution*, vol. 12, no. 9, pp. 2072–2085, May 2018, doi: 10.1049/iet-gtd.2017.1203.

[11] I. A. Chidambaram and B. Paramasivam, "Optimized load-frequency simulation in restructured power system with redox flow batteries and interline power flow controller," *International Journal of Electrical Power and Energy Systems*, vol. 50, pp. 9–24, Sep. 2013, doi: 10.1016/j.ijepes.2013.02.004.

[12] A. Daraz, S. A. Malik, H. Mokhlis, I. U. Haq, F. Zafar, and N. N. Mansor, "Improved-fitness dependent optimizer based FOI-PD controller for automatic generation control of multi-source interconnected power system in deregulated environment," *IEEE Access*, vol. 8, pp. 197757–197775, 2020, doi: 10.1109/ACCESS.2020.3033983.

[13] K. Jagatheesan, B. Anand, S. Samanta, N. Dey, A. S. Ashour, and V. E. Balas, "Design of a proportional-integral-derivative controller for an automatic generation control of multi-area power thermal systems using firefly algorithm," *IEEE/CAA Journal of Automatica Sinica*, vol. 6, no. 2, pp. 503–515, Mar. 2019, doi: 10.1109/JAS.2017.7510436.

[14] V. L. Chuong, N. H. Nam, L. H. Giang, and T. N. L. Vu, "Robust fractional-order PI/PD controllers for a cascade control structure of servo systems," *Fractal and Fractional*, vol. 8, no. 4, p. 244, Apr. 2024, doi: 10.3390/fractalfract8040244.

[15] A. Mukhtar, P. M. Tiwari, S. Alotaibi, T. Alzahrani, B. Namomsa, and M. Ahmed, "Optimal design of tilt integral derivative controller for a boost converter based on swarm-inspired algorithms," *Scientific Reports*, vol. 15, no. 1, p. 57, Jan. 2025, doi: 10.1038/s41598-024-84088-7.

[16] E. Çelik and N. Öztürk, "Novel fuzzy 1PD-TI controller for AGC of interconnected electric power systems with renewable power generation and energy storage devices," *Engineering Science and Technology, an International Journal*, vol. 35, p. 101166, Nov. 2022, doi: 10.1016/j.jestch.2022.101166.

[17] V. T. Nguyen, T. L.-T. Tran, D. H. Tuan, D. C. Hien, V. P. Nguyen, and V. V. Huynh, "Load frequency control for integrated hydro and thermal power plant power system," *International Journal of Electrical and Computer Engineering (IJECE)*, vol. 15, no. 4, p. 3583, Aug. 2025, doi: 10.11591/ijece.v15i4.pp3583-3592.

[18] N. R. Babu *et al.*, "Enhanced automatic generation control in multiarea power systems: crow search optimized cascade FOPI-TIDDN controller with integrated renewable solar thermal models and HVDC lines," *Engineering Reports*, vol. 7, no. 5, May 2025, doi: 10.1002/eng2.70185.

[19] N. R. Babu, L. C. Saikia, S. K. Bhagat, and A. Saha, "Maiden application of hybrid crow-search algorithm with particle swarm optimization in LFC studies," *Proceedings of International Conference on Artificial Intelligence and Applications*, 2021, pp. 427–439, doi: 10.1007/978-981-15-4992-2_40.
[20] E. A. Jiya and I. B. Oluwafemi, "Advanced genetic algorithm (GA)-independent component analysis (ICA) ensemble model for predicting trapped humans through hybrid dimensionality reduction," *Scientific African*, vol. 27, p. e02564, Mar. 2025, doi: 10.1016/j.sciaf.2025.e02564.
[21] O. Roeva, D. Zoteva, G. Roeva, and V. Lyubenova, "An efficient hybrid of an ant lion optimizer and genetic algorithm for a model parameter identification problem," *Mathematics*, vol. 11, no. 6, p. 1292, Mar. 2023, doi: 10.3390/math11061292.
[22] Q. Yang, H. Huang, J. Zhang, H. Gao, and P. Liu, "A collaborative cuckoo search algorithm with modified operation mode," *Engineering Applications of Artificial Intelligence*, vol. 121, p. 106006, May 2023, doi: 10.1016/j.engappai.2023.106006.
[23] X.-B. Meng, X. Z. Gao, L. Lu, Y. Liu, and H. Zhang, "A new bio-inspired optimisation algorithm: bird swarm algorithm," *Journal of Experimental & Theoretical Artificial Intelligence*, vol. 28, no. 4, pp. 673–687, Jul. 2016, doi: 10.1080/0952813X.2015.1042530.
[24] S. K. Bhagat, L. C. Saikia, and N. R. Babu, "Effect of partial loading on a three-area hydro-thermal system integrated with realistic dish-stirling solar thermal system, accurate model of high-voltage direct link considering virtual inertia and energy storage systems," *International Transactions on Electrical Energy Systems*, vol. 31, no. 12, Dec. 2021, doi: 10.1002/2050-7038.13169.
[25] S. K. Bhagat, L. C. Saikia, and N. R. Babu, "Inertia emulation control strategy of an accurate model of HVDC link in a multi-area automatic generation control system integrated precise wind turbine system," *Iranian Journal of Science and Technology, Transactions of Electrical Engineering*, vol. 48, no. 1, pp. 143–163, Mar. 2024, doi: 10.1007/s40998-023-00641-6.

BIOGRAPHIES OF AUTHORS

Rambabu Kasukurthi is a research scholar in the Department of Electrical Engineering at the College of Engineering, Andhra University. He holds an M.Tech. degree in power systems from Acharya Nagarjuna University, Guntur. His research interests include power systems and smart grids. He has published several research papers on topics such as, demand-side management using machine learning and IoT-enabled smart power systems. He can be contacted at email: rambabu.kasukurthi@gmail.com.

Dr. R. Srinu Naik is an associate professor in the Department of Electrical Engineering at the College of Engineering, Andhra University. He earned his Ph.D. from the same university with a specialization in power systems, electrical earthing, and non-conventional energy systems. With over 25 years of academic experience, he has served in various roles, ranging from teaching assistant to assistant professor and associate professor. He has successfully guided doctoral research, published numerous research articles, book chapters, and books, and continues to contribute actively to advancements in power engineering and renewable energy. He can be contacted at email: naiknaiknaik@gmail.com.